A new numerical treatment of moving wet/dry fronts in dam-break flows

Alia Al-Ghosoun* Michael Herty† Mohammed Seaid‡

Abstract

The aim of this paper is to present a new finite volume method for moving wet/dry fronts in shallow water flows. The method consists on reformulating the shallow water equations in a moving wetted domain where the wet/dry interface is located using the speed of the water flow. A set of parametrized coordinates is introduced and the underlying equations are transformed to a new hyperbolic system with advection terms to be solved in fixed domains. A well-balanced finite volume method is developed to approximate numerical solutions of the parametrized system. We derive a well-balanced approximation of the source terms and prove that the proposed method is well-balanced for the shallow water flows in the presence of moving wet/dry fronts over non-flat topography. Several numerical results confirm the reliability and accuracy of the new method.

Keywords. Shallow water equations; Wet/dry fronts; Finite volume method; Well-balanced discretization; Dam-break problems

1 Introduction

Nonlinear shallow water equations are typically used to model free-surface flows, river and lake hydrodynamics, and long wave run-up, as well as flows in open channels, lakes, reservoirs, coastal areas, estuaries and harbors among others [22, 9]. Many of these applications involve moving fronts in which wetting and drying over variable topography occurs, and numerically solving these processes is becoming increasingly important. For instance, predictions of flooding due to a storm surge, breached dam, or overtopped levee are crucial for disaster planning. Wave run-up estimates are needed for beach and coastal structure design [24, 19]. Descriptions of inundation, in both estuarine tidal flats and riverine flood plains, are also key for predicting the transport of suspended and dissolved substances. The hydrodynamics of shallow water flows on wetting and drying areas is of great interest in a wide range of physical flows. The basic feature of these flows is that the vertical scale is much smaller than a typical horizontal scale. Such shallow water flows give rise to challenging problems in both theoretical analysis and numerical simulation. Numerical simulations of shallow water models have been devoted a lot of efforts so far, and as a consequence, many numerical models have been developed for scientific researches and engineering applications. In real case simulations, treatment of moving wet/dry fronts is getting more and more popular in the hydraulics community to represent the complex flow features at river banks and coastal lines.

*School of Engineering and Computing Sciences, University of Durham, South Road, Durham DH1 3LE, UK *E-mail:* alia.r.al-ghosoun@durham.ac.uk

†RWTH Aachen University, IGPM, Templergraben 55, D-52056 Aachen, Germany *E-mail:* herty@igpm.rwth-aachen.de

‡School of Engineering and Computing Sciences, University of Durham, South Road, Durham DH1 3LE, UK *E-mail:* m.seaid@durham.ac.uk

The numerical approximation of water flows over wetting and drying areas requires important choices and compromises to be made when simulations of the water flow are carried out. These compromises are necessary to minimize both artificial numerical dissipation and dispersion. The resulting numerical dissipation may severely damp the free-surface flow, producing exaggerated inaccurate results, whereas the artificial numerical dispersion may introduce nonphysical oscillations known by wiggles. In general, conservative Eulerian algorithms such as those based on finite volume shock-capturing techniques perform very well when applied to shallow water flows over fully wetted areas, see for example [26]. However, when such an algorithm is employed to solve shallow water flows over wetting and drying areas, numerical inaccuracies usually occur at the wet/dry interfaces due to the loss of entropy property in the discretization. To overcome this difficulty, many techniques and methods have been developed in the past two decades with an even increasing interest, see for instance [26, 12, 1, 6, 7, 11, 13, 17, 20, 21, 29, 10, 5, 18, 14] and further references are therein. Among them, some of the resultant algorithms may not maintain the conservation property in the process of enforcing states at the moving wet/dry interface so as to suppress any undesired numerical oscillations. The objective of this study is to devise a stable, monotone and accurate numerical method able to approximate solutions to shallow water flows over wetting and drying areas.

In this paper, we propose a new numerical model for moving wet/dry fronts in shallow water equations using the parameterization concept and the point-wise Riemann solver. In the current model, we reformulate the nonlinear shallow water equations in a new set of moving coordinates, and treat them as the model variables to be predicted at every time step. To numerically solve the modified equations we consider a well-balanced finite volume method. The object of the current work is to develop a numerical approach able to accurately approximate solutions to moving wet/dry fronts in shallow water flows. Our aim is to develop a class of numerical methods that are simple, easy to implement, and accurately solves the moving wet/dry fronts in shallow water flows without relying on complicated techniques. The proposed finite volume method can be interpreted as a fractional-stage scheme. In the first stage, the transport terms are solved by integrating the system along the characteristics defined by the interface velocity, while the numerical solutions are computed through a finite volume formulation of flux form in the second stage. The main features of such a finite volume scheme are on one hand, the capability to satisfy the conservation property resulting in numerical solutions free from spurious oscillations in significant moving wet/dry fronts, and on the other hand the achievement of strong stability for simulations of slowly varying wet/dry interfaces as well as rapidly varying wet/dry interfaces containing also shocks or discontinuities. Moreover, the numerical formulation is devised so that the source terms are well balanced to the fluxes on the discretized level. These features are verified using several test examples of shallow water flows over wetting and drying areas. Results presented in this paper show high resolution of the proposed techniques and permit the straightforward application of the method to more complex, physically based shallow water flows.

This paper is structured as follows. In section 2 we present the problem statement for moving wet/dry fronts in shallow water flows. Numerical solution of the parametrized shallow water equations is formulated in section 4. This section includes the finite volume discretization of the system and the solution of the moving fronts. Section 5 is devoted to numerical results for several test examples in shallow water flows. Concluding remarks end the paper in section 6.

2 Equations for wet/dry fronts in shallow water flows

The shallow water equations can be derived by depth-averaging the Navier-Stokes equations, neglecting the vertical acceleration of water particles, and taking the pressure distribution to be

hydrostatic, see [11, 26] among others. In one space dimension, ignoring viscous terms and surface stresses, the shallow water equations read

$$\begin{aligned} \frac{\partial h}{\partial t} + \frac{\partial (hu)}{\partial x} &= 0, & x \in [a,b], \\ \frac{\partial (hu)}{\partial t} + \frac{\partial}{\partial x}\left(hu^2 + \frac{1}{2}gh^2\right) &= -gh\frac{\partial z}{\partial x}, & x \in [a,b], \end{aligned} \tag{2.1a}$$

where $[a,b]$ is the computational domain, $z(x)$ is the function characterizing the bottom topography, $h(t,x)$ is the height of the water above the bottom, g is the acceleration due to gravity, $u(t,x)$ is the flow velocity. The equations (2.1a) have been widely used to model water flows, flood waves, dam-break problems, and have been studied in a number of books and papers, see for instance [22, 26, 9, 16]. Computing their numerical solutions is not trivial due to the nonlinearity in the flux function, the presence of the convective terms, and the coupling of the equations through the source term. In many applications, the solutions of equations (2.1a) present steep fronts and even discontinuities, which need to be resolved accurately in applications and often cause severe numerical difficulties, compare [16, 26]. In the current study we are interested in moving wet/dry fronts in shallow water flows for which the equations (2.1a) are solved subject to the following initial conditions

$$h(0,x) = \begin{cases} h_0, & \text{if} \quad x \le x_0, \\ \\ 0, & \text{if} \quad x > x_0, \end{cases} \qquad u(0,x) = u_0, \tag{2.1b}$$

where $x_0 \in [a,b)$ is the initial location of the wet/dry interface, h_0 and u_0 are given water height and water velocity, respectively. Note that most of numerical methods for solving the equations (2.1) perturb the dry state (zero water height) using a wetted threshold above which the solution state is considered to be dry. This is mainly used to avoid division by zero for updating the water velocity during the simulation process. However, perturbing the water height may result in inaccuracy in the computed solutions and may lead to false location of the wet/dry fronts on the coastal zones. Furthermore, if due to numerical oscillations the water height h becomes negative, the calculation will simply break down.

In the present work we propose an alternative formulation of the equations (2.1) to deal with wet/dry fronts. The idea consists on rewriting the shallow water equations in a moving domain and solve the obtained model only for the wetted area. The advection of the wet/dry interface is achieved by using the speed of the water. Hence, the problem statement becomes: solve the system

$$\begin{aligned} \frac{\partial h}{\partial t} + \frac{\partial (hu)}{\partial x} &= 0, & x \in \Big[a, \xi(t)\Big], \\ \frac{\partial (hu)}{\partial t} + \frac{\partial}{\partial x}\left(hu^2 + \frac{1}{2}gh^2\right) &= -gh\frac{\partial z}{\partial x}, & x \in \Big[a, \xi(t)\Big], \end{aligned} \tag{2.2a}$$

where the interface $\xi(t)$ is defined by the ordinary differential equation

$$\begin{aligned} \dot{\xi}(t) := \frac{d\xi(t)}{dt} &= s, \\ \xi(0) &= x_0, \end{aligned} \tag{2.2b}$$

for a given speed s. Based on the analysis reported in [25], for the application to a moving wet/dry interface the maximal speed of the flow propagation in the shallow water system is bounded by $|u| + 2\sqrt{g\,h}$. Therefore a possible choice for capturing all information in the domain $[a, \xi(t)]$ is simply

$$s = |u| + 2\sqrt{g\,h}. \tag{2.3}$$

In general, other velocities s might be used to move the front in the computational domain which allows also to decouple the solution of the equations (2.2a) and (2.2b).

REMARK **2.1** *Consider the shallow water equations* (2.1a) *equipped with the initial data* (2.1b). *The solution to this Riemann problem consists of a one-rarefaction wave. The speed at the interface* x_0 *is therefore* $u_0 + 2\sqrt{gh_0}$.

It is clear that the shallow water equations (2.2) have to be solved in a time-dependent computational domain requiring a mesh at each time step. In order to avoid this difficulty we perform a change of coordinates. Thus, we define the new coordinates (t, y)

$$t = t, \qquad y = \frac{x - a}{\xi(t) - a},$$

and the new solution variables in the transformed coordinate system as

$$\begin{aligned} H(t,y) &= h\Big(t, y\big(\xi(t) - a\big) + a\Big), \\ U(t,y) &= u\Big(t, y\big(\xi(t) - a\big) + a\Big), \\ Z(t,y) &= z\Big(t, y\big(\xi(t) - a\big) + a\Big). \end{aligned} \tag{2.4}$$

Hence, after some algebra, the shallow water equations (2.2a) transform to

$$\begin{aligned} \frac{\partial H}{\partial t} - \frac{\dot{\xi} y}{\xi - a}\frac{\partial H}{\partial y} + \frac{1}{\xi - a}\frac{\partial (HU)}{\partial y} &= 0, && y \in [0,1], \\ \frac{\partial (HU)}{\partial t} - \frac{\dot{\xi} y}{\xi - a}\frac{\partial (HU)}{\partial y} + \frac{1}{\xi - a}\,\frac{\partial}{\partial y}\left(HU^2 + \frac{1}{2}gH^2\right) &= -g\frac{H}{\xi - a}\frac{\partial Z}{\partial y}, && y \in [0,1]. \end{aligned} \tag{2.5}$$

Note that the above equations for (H, HU) are now defined in the fixed domain $(t, y) \in \mathbb{R}^+ \times [0, 1]$. The transformation is well-defined provided that $\xi(0) > a$ and $s \geq 0$. These conditions are satisfied for the case of a moving front in a dry area. Furthermore, boundary conditions at $x = a$ are not affected by this transformation. Introducing the advective derivative of any physical variable w as

$$\frac{Dw}{Dt} = \frac{\partial w}{\partial t} - \frac{\dot{\xi}\, y}{\xi - a}\frac{\partial w}{\partial y}, \tag{2.6}$$

the shallow water equations (2.5) reduce for $y \in [0, 1]$ to

$$(\xi - a)\frac{DH}{Dt} + \frac{\partial (HU)}{\partial y} = 0, \tag{2.7a}$$

$$(\xi - a)\frac{D(HU)}{Dt} + \frac{\partial}{\partial y}\left(HU^2 + \frac{1}{2}gH^2\right) = -gH\frac{\partial Z}{\partial y}. \tag{2.7b}$$

For simplicity in the presentation we also rewrite the equations (2.7) in a conservative form as

$$(\xi - a)\frac{D\mathbf{W}}{Dt} + \frac{\partial \mathbf{F}(\mathbf{W})}{\partial y} = \mathbf{S}(\mathbf{W}), \tag{2.8}$$

where

$$\mathbf{W} = \begin{pmatrix} H \\ HU \end{pmatrix}, \qquad \mathbf{F}(\mathbf{W}) = \begin{pmatrix} HU \\ HU^2 + \frac{1}{2}gH^2 \end{pmatrix}, \qquad \mathbf{S}(\mathbf{W}) = \begin{pmatrix} 0 \\ -gH\dfrac{\partial Z}{\partial y} \end{pmatrix}.$$

It should be stressed that, the solution of the parametrized equations (2.7) is to be computed in a fixed domain $[0,1]$. In addition, the system (2.7) retains the same structure for the physical fluxes as the original shallow water equations (2.1a). Remark that once the solution (H,U) of the system (2.7) and (2.2b) is computed, the solution (h,u) of the system (2.1) can easily be recovered using the transformation (2.4). It is also well-known that modification of conservation laws lead to changes in shock speed, see for example [15]. Here, the eigenvalues of the transformed system in the convective variables are

$$\lambda_1 = \frac{u-\sqrt{gh}}{\xi - a}, \qquad \lambda_2 = \frac{u+\sqrt{gh}}{\xi - a}. \tag{2.9}$$

Clearly, if the front speed $s = 0$ then the transformation simply scales the computational domain in the space coordinates but not in the time variable. In the simplest case of a linear advection equation for fixed (positive) velocity u

$$\frac{\partial h}{\partial t} + u\frac{\partial h}{\partial x} = 0, \qquad h(t,0) = h_0(t),$$

we can easily verify that the solution to the advection equation with compactly supported initial data $h_0(x)$ in $[0,\xi(t)]$ with $\xi'(t) > 0$ and $\xi(0) > 0$ coincides with the solution $H(t,y)$ to the parametrized equation

$$\frac{\partial H}{\partial t} - \frac{\xi'(t)y}{\xi}\frac{\partial H}{\partial y} + \frac{u}{\xi}\frac{\partial H}{\partial y} = 0, \qquad H(t,0) = h_0(t),$$

where $H(0,y) = h_0\left(y\xi(0)\right)$. It should also be noted that the new parametrized system (2.7) satisfies the still-water equilibrium. Recall that for the steady state with still water $u(t,x) = 0$, the momentum equation in the original system (2.1a) yields

$$h(t,x) + z(x) = c, \tag{2.10}$$

where c is a positive constant. This property (known by C-property) is needed to be preserved at the discrete level to reconstruct a well-balanced method [4]. A possibility to derive a well-balanced scheme introduced by [6] is to rewrite the equations (2.2) in terms of the total height $\eta(t,x) = h(t,x)+z(x)$. A similar procedure may be applied in the parametrized system (2.7). Let us consider the rescaled water height $H(t,y)$ and the rescaled water discharge $Q(t,y) = H(t,y)U(t,y)$, and define the total water depth $\nu(t,y)$ as

$$\nu(t,y) = \eta\big(t, y\left(\xi(t)-a\right)+a\big) = h\big(y\left(\xi(t)-a\right)+a\big) + z\big(y\left(\xi(t)-a\right)+a\big) = H(t,y) + Z(t,y).$$

Hence, at still water equilibrium $U(t,y) = 0$, the parametrized system (2.7) reduces to

$$\begin{aligned} -y\dot{\xi}\frac{\partial}{\partial y}H(t,y) &= 0, \\ \frac{1}{2}\frac{\partial}{\partial y}\left(gH^2(t,y)\right) &= -gH(t,y)\frac{\partial}{\partial y}Z(t,y). \end{aligned}$$

Since at the steady state $\dfrac{d\xi}{dt} = 0$, we obtain

$$H(t,y) + Z(t,y) = C, \tag{2.11}$$

where C is a positive constant. Thus, the proposed transformation preserves the hydrostatic reconstruction and in the case $u(t,x) = 0$ we may use the same techniques to develop a well-balanced discretization. Note however, that in a finite volume method for the rescaled equations (2.7) one needs to account for the additional temporal dependence of the bottom profile due to the rescaled bed $Z(t,y) = z(y(\xi(t)-a)+a)$.

3 Well-balanced finite volume methods

To approximate numerical solutions of the shallow water equations (2.7) we consider a class of well-balanced finite volume discretizations using the different methods to reconstruct the numerical fluxes. This method is adapted according to the parametrized equations (2.7) including advective terms and the modified bottom beds. The presented methods use an operator splitting where the transport part and the conservation part are treated separately. The major part of this section is devoted to the treatment of the source terms in (2.7) using additional corrections to obtain a well-balanced finite volume method. The numerical method we propose for approximating solutions to equations (2.8) can be interpreted as a fractional step technique where the advective part is decoupled from the conservative part in the temporal discretization. Thus, at each time step the new water height and discharge are updated by first solving the advective equation

$$(\xi - a)\,\frac{D\mathbf{W}}{Dt} = 0, \tag{3.1}$$

then the conservation system

$$\frac{\partial \mathbf{W}}{\partial t} + \frac{\partial \mathbf{F}(\mathbf{W})}{\partial y} = \mathbf{S}(\mathbf{W}). \tag{3.2}$$

We discretize the space domain in cells $[y_{i-\frac{1}{2}}, y_{i+\frac{1}{2}}]$ with same length Δy for sake of simplicity. We also divide the time interval into subintervals $[t_n, t_{n+1}]$ with uniform size Δt. Here, $t_n = n\Delta t$, $y_{i-\frac{1}{2}} = i\Delta y$ and $y_i = (i + \frac{1}{2})\Delta y$ is the center of the control volume. We use the notation $w_i(t)$ to denote the space average of a function $w = w(t, x)$ in the cell $[y_{i-\frac{1}{2}}, y_{i+\frac{1}{2}}]$ at time t, by $w_i^n = w_i(t^n)$, and by $w_{i+\frac{1}{2}}$ to denote the numerical flux at $y = y_{i+\frac{1}{2}}$ and time t,

$$w_i(t) = \frac{1}{\Delta y}\int_{y_{i-\frac{1}{2}}}^{y_{i+\frac{1}{2}}} w(y,t)dy, \qquad w_{i+\frac{1}{2}} = w(y_{i+\frac{1}{2}}, t).$$

To solve the advection equation (3.1) two steps are required namely, the computation of characteristic trajectories and the interpolation procedure. Both steps are crucial to the overall accuracy of the method of characteristics. For each mesh point $y_{i+\frac{1}{2}}$ the characteristic curves $Y_{i+\frac{1}{2}}$ associated with (2.6) are the solutions of the initial-value problem

$$\begin{aligned} \frac{dY_{i+\frac{1}{2}}(\tau)}{d\tau} &= v_{i+\frac{1}{2}}\Big(\tau, Y_{i+\frac{1}{2}}(\tau)\Big), \qquad \tau \in [t_n, t_{n+1}]\,, \\ Y_{i+\frac{1}{2}}(t_{n+1}) &= y_{i+\frac{1}{2}}, \end{aligned} \tag{3.3}$$

where $v(\tau, y) = -\dfrac{\dot{\xi}(\tau)y}{\xi(\tau) - a}$. Note that $Y_{i+\frac{1}{2}}(\tau)$ is the departure point at time τ of a particle that will arrive at gridpoint $y_{i+\frac{1}{2}}$ in time t_{n+1}. Note that the method of characteristics does not follow the flow particles forward in time, as the Lagrangian methods do, instead it traces backwards the position at time t_n of particles that will reach the points of a fixed mesh at time t_{n+1}. The solutions of (3.3) can be expressed as

$$Y_{i+\frac{1}{2}}(t_n) = y_{i+\frac{1}{2}} - \int_{t_n}^{t_{n+1}} v_{i+\frac{1}{2}}\left(\tau, Y_{i+\frac{1}{2}}(\tau)\right) d\tau. \tag{3.4}$$

For a velocity field explicitly given independent of the solution, the integral in (3.4) can be determined analytically. In other general cases, this integral can be calculated using a second-order extrapolation based on the mid-point rule which is accurate enough to maintain a particle on its curved trajectory. More details on these techniques can be found [23] among others.

Once the characteristics curves $Y(t_n)$ are known, the method of characteristics advects the solution of (2.7) at instant t_{n+1} as

$$\widehat{\mathbf{W}}(t_{n+1}, y) := \mathbf{W}\left(t_n, Y(t_n)\right). \tag{3.5}$$

Note that the advection equation (3.1) can also be solved by assuming that its exact solution in an unbounded domain is given by

$$\mathbf{W}(t, y) = \mathbf{W}_0\left(y\frac{\xi(t)}{\xi(0)}\right),$$

where $\mathbf{W}_0$ is the initial condition associated with the system (2.8). Hence, the exact solution to the advection equation in the time interval $[t_n, t_{n+1}]$ is

$$\widehat{\mathbf{W}}_i^n := \mathbf{W}^n\left(y_i\frac{\xi^{n+1}}{\xi^n}\right). \tag{3.6}$$

Notice that in general, the departure points $Y(t_n)$ do not coincide with the spatial position of a gridpoint. Assuming a suitable approximation is made for $Y(t_n)$, the solution $\widehat{\mathbf{W}}(t_{n+1}, y)$ in (3.5) should be obtained by interpolation from known values at the gridpoints in the host cell of the departure points. The interpolation procedure we used in this paper is the cubic spline interpolation most commonly used in practice. Other interpolation procedures can also be applied.

Integrating equations (2.8) along the characteristics with respect to time and space over the time-space control domain $[t_n, t_{n+1}] \times [y_{i-\frac{1}{2}}, y_{i+\frac{1}{2}}]$ we obtain the following discrete equation

$$\mathbf{W}_i^{n+1} = \widehat{\mathbf{W}}_i^n - \frac{\Delta t}{\Delta y}\left(\widehat{\mathbf{F}}_{i+\frac{1}{2}}^n - \widehat{\mathbf{F}}_{i-\frac{1}{2}}^n\right) + \frac{\Delta t}{\Delta y}\int_{y_i-\frac{1}{2}}^{y_i+\frac{1}{2}} \mathbf{S}(\widehat{\mathbf{W}}^n)\, dy, \tag{3.7}$$

where $\widehat{\mathbf{F}}_{i\pm\frac{1}{2}}^n = \mathbf{F}\left(\widehat{\mathbf{W}}_{i\pm\frac{1}{2}}^n\right)$ are the numerical fluxes at $y = y_{i\pm\frac{1}{2}}$ and time $t = t_n$. The spatial discretization (3.7) is complete when a numerical construction of the fluxes and source terms are chosen. In general this step can be carried out using any finite volume method developed in the literature for solving hyperbolic systems of conservation laws, see for example [15, 26]. In the current study we consider the following methods:

Lax-Friedrichs method [27]:

$$\widehat{\mathbf{F}}_{i+\frac{1}{2}}^n = \frac{1}{2}\left(\mathbf{F}\left(\widehat{\mathbf{W}}_{i+1}^n\right) + \mathbf{F}\left(\widehat{\mathbf{W}}_i^n\right)\right) + \frac{\Delta y}{2\Delta t}\left(\widehat{\mathbf{W}}_i^n - \widehat{\mathbf{W}}_{i+1}^n\right). \tag{3.8}$$

Rusanov method [8]:

$$\widehat{\mathbf{F}}_{i+\frac{1}{2}}^n = \frac{1}{2}\left(\mathbf{F}\left(\widehat{\mathbf{W}}_{i+1}^n\right) + \mathbf{F}\left(\widehat{\mathbf{W}}_i^n\right)\right) + \frac{1}{2}\lambda\left(\widehat{\mathbf{W}}_i^n - \widehat{\mathbf{W}}_{i+1}^n\right), \tag{3.9}$$

where the Rusanov speed is defined as $\lambda = \max\left(\lambda_1^n, \lambda_2^n\right)$.

Roe method [21]:

$$\widehat{\mathbf{F}}_{i+\frac{1}{2}}^n = \frac{1}{2}\left(\mathbf{F}\left(\widehat{\mathbf{W}}_{i+1}^n\right) + \mathbf{F}\left(\widehat{\mathbf{W}}_i^n\right)\right) + \frac{1}{2}\mathbf{A}\left(\widehat{\mathbf{W}}_{i+\frac{1}{2}}^n\right)\left(\widehat{\mathbf{W}}_i^n - \widehat{\mathbf{W}}_{i+1}^n\right), \tag{3.10}$$

where the averaged state $\widehat{\mathbf{W}}^n_{i+\frac{1}{2}}$ is calculated as

$$\widehat{\mathbf{W}}^n_{i+\frac{1}{2}} = \begin{pmatrix} \dfrac{\widehat{h}^n_i + \widehat{h}^n_{i+1}}{2} \\ \dfrac{\sqrt{\widehat{h}^n_i}\,\widehat{u}^n_i + \sqrt{\widehat{h}^n_{i+1}}\,\widehat{u}^n_{i+1}}{\sqrt{\widehat{h}^n_i} + \sqrt{\widehat{h}^n_{i+1}}} \end{pmatrix}, \tag{3.11}$$

and the Roe matrix $\mathbf{A} = \mathbf{R}\mathbf{\Lambda}\mathbf{R}^{-1}$ with

$$\mathbf{R} = \begin{pmatrix} 1 & 1 \\ \widehat{\lambda}_1 & \widehat{\lambda}_2 \end{pmatrix}, \qquad \mathbf{\Lambda} = \begin{pmatrix} \widehat{\lambda}_1 & 0 \\ 0 & \widehat{\lambda}_2 \end{pmatrix},$$

where $\widehat{\lambda}_1$ and $\widehat{\lambda}_2$ are the eigenvalues in (2.9) calculated at the averaged state (3.11).

FVC method [3]: To reconstruct the numerical fluxes using the finite volume characteristics method, the equations (3.2) are first reformulated in an advective form as

$$\begin{aligned} \frac{\partial H}{\partial t} + U\frac{\partial H}{\partial y} &= -H\frac{\partial U}{\partial y}, \\ \frac{\partial U}{\partial t} + U\frac{\partial U}{\partial y} &= -gH\frac{\partial\,(H+Z)}{\partial y}. \end{aligned} \tag{3.12}$$

Then, the associated characteristic curves $X_{i+\frac{1}{2}}(\tau)$ are computed as

$$\begin{aligned} \frac{dX_{i+\frac{1}{2}}(\tau)}{d\tau} &= U\Big(\tau, X_{i+\frac{1}{2}}(\tau)\Big), \quad \tau \in [t_n, t_n + \Delta t], \\ X_{i+\frac{1}{2}}(t_n + \Delta t) &= x_{i+\frac{1}{2}}. \end{aligned} \tag{3.13}$$

The initial-value problem (3.13) is solved using the same algorithm as the one used for solving the equations (3.3). The numerical fluxes in the FVC schemes are obtained by integrating the advective equations (3.12) along the characteristics in the time interval $[t_n, t_n + \Delta t]$. Assume an accurate approximation of the characteristics curves $X_{i+\frac{1}{2}}(t_n)$ is made, the intermediate solutions are obtained from (3.12) as

$$\begin{aligned} H^n_{i+\frac{1}{2}} &= \widetilde{H}^n_{i+\frac{1}{2}} - \frac{\Delta t}{\Delta y}\widetilde{H}^n_{i+\frac{1}{2}}\left(U^n_{i+1} - U^n_i\right), \\ U^n_{i+\frac{1}{2}} &= \widetilde{U}^n_{i+\frac{1}{2}} - g\frac{\Delta t}{\Delta y}\left((H^n + Z)_{i+1} - (H^n + Z)_i\right), \end{aligned} \tag{3.14}$$

where

$$\widetilde{H}^n_{i+\frac{1}{2}} = H\left(t_n, X_{i+\frac{1}{2}}(t_n)\right), \qquad \widetilde{U}^n_{i+\frac{1}{2}} = U\left(t_n, X_{i+\frac{1}{2}}(t_n)\right),$$

are the solutions at the characteristic foot computed by interpolation from the gridpoints of the control volume where the departure point $X_{i+\frac{1}{2}}(t_n)$ belongs. Hence, the numerical fluxes for the FVC method are defined by

$$\widehat{\mathbf{F}}^n_{i+\frac{1}{2}} = \mathbf{F}\left(\widehat{\mathbf{W}}^n_{i+\frac{1}{2}}\right), \tag{3.15}$$

with the intermediate state $\widehat{\mathbf{W}}^n_{i+\frac{1}{2}}$ is given

$$\widehat{\mathbf{W}}^n_{i+\frac{1}{2}} = \begin{pmatrix} H^n_{i+\frac{1}{2}} \\ \\ U^n_{i+\frac{1}{2}} \end{pmatrix}.$$

It should be stressed that the Lax-Friedrichs, Rusanov and Roe methods have been widely used for the numerical solution of shallow water equations whereas, the FVC method has been recently proposed in [3]. Analysis of the FVC method and numerical comparison of its performance compared to Rusanov and Roe methods can also be found in [2].

4 Treatment of source terms

Obviously the above method is first-order accurate for any first-order discretization of the source term in (3.7). In order to motivate the derivation of the additional source terms necessary for well-balancing the discretization of gradient fluxes and source terms we first consider the simple case with $\frac{d\xi}{dt} = 0$, $\xi = 1$ and $a = 0$. Then, the system (2.7) and the equation (2.5) coincide and many approaches to well-balancing are known, see for example [4, 17, 1, 20, 12, 7]. In the current study, to develop a well-balanced scheme method we resolve the steady-state dynamics up to high order. Thus, for still water equilibrium the conservation property (2.11) is preserved at time t_n *i.e.*,

$$U^n_i = 0, \qquad H^n_i + Z^n_i = C,$$

where C is a constant and $Z^n_i = Z\left(y_i\xi(t^n)\right) = Z(y_i)$. A Taylor expansion up to order $\mathcal{O}(\Delta y^3)$ yields

$$H^{n+1}_i - H^n_i = \frac{1}{2}\Delta y^2 (H_{yy})^n_i = -\frac{1}{2}\Delta y^2 (Z_{yy})^n_i + \mathcal{O}(\Delta y^3),$$

and assuming that the source term in (3.7) is integrated by mid-point rule a similar computation leads to

$$(HU)^{n+1}_i - (HU)^n_i = \mathcal{O}(\Delta y^3).$$

Hence, for a flow at rest the discretization (3.7) preserves the steady-state property up to the order $\mathcal{O}(\Delta y^3)$ provided that the additional term $\mathcal{S}^n_i = \frac{1}{2}\Delta y^2 (Z_{yy})^n_i$ is added to the equation of conservation of mass. Note that far from the steady-state, including the source term $\mathcal{S}^n_i$ would not change the properties of the scheme since this additional term is below the resolution of the considered finite volume methods.

In the general case with $\frac{d\xi}{dt} \neq 0$ we proceed in a similar manner to construct a well-balanced discretization for the system (2.7). Here, for simplicity in the derivations we assume $a = 0$ and the equations (2.7) reduce to

$$\begin{aligned} \frac{\partial H}{\partial t} - \frac{\dot{\xi} y}{\xi}\frac{\partial H}{\partial y} + \frac{1}{\xi}\frac{\partial Q}{\partial y} &= 0, \\ \frac{\partial Q}{\partial t} - \frac{\dot{\xi} y}{\xi}\frac{\partial Q}{\partial y} + \frac{1}{\xi}\frac{\partial M}{\partial y} &= -g\frac{H}{\xi}\frac{\partial Z}{\partial y}, \end{aligned} \tag{4.1}$$

where $Q = HU$ and $M = HU^2 + \frac{1}{2}gH^2$. Note that unlike the previous case with $\frac{d\xi}{dt} = 0$, the scaled bottom bed in (4.1) depends on the time variable as $Z(t, y) = z(y\xi(t))$ with $z(x)$ describes the

original bottom topography in (2.5). For still water equilibrium the conservation property (2.11) should be preserved *i.e.*,

$$U(t,y) = 0, \qquad H + Z = H(t,y) + z\left(y\xi(t)\right) = C.$$

As in the previous case we seek a discretization of the source term in (3.7) such that

$$H_i^{n+1} = C - z\left(y_i\xi^{n+1}\right) + \mathcal{O}(\Delta y^3) \qquad \text{and} \qquad Q_i^{n+1} - Q_i^n = \mathcal{O}(\Delta y^3).$$

A Taylor expansion in y of $\widehat{H}_i$ leads to

$$\widehat{H}_i = H_i^n + \Delta t (H_y)_i^n \frac{y_i\xi'(t^n)}{\xi(t^n)} + \frac{\Delta t^2}{2}(H_{yy})_i^n \left(\frac{y_i\xi'(t^n)}{\xi(t^n)}\right)^2 + \frac{\Delta t^2}{2}(H_y)_i^n \frac{y_i\xi''(t^n)}{\xi(t^n)} + \mathcal{O}(\Delta y^3),$$

with a similar expansion for the water discharge $\widehat{Q}_i$. The Taylor expansion of Z is given by

$$Z_i^{n+1} := z(y_i\xi(t_n + \Delta t)) = Z_i^n + \Delta t (z_x)_i^n y_i\xi'(t^n) + \frac{\Delta t^2}{2}(z_{xx})_i^n y_i^2(\xi'(t^n))^2 + \frac{\Delta t^2}{2} y_i\xi''(t^n) + \mathcal{O}(\Delta y^3).$$

For example, using the Lax-Friedrichs method (3.8), the discretization of the balance law (3.2) is given by

$$\begin{aligned}
H_i^{n+1} - \widehat{H}_i &= \frac{1}{2}\left(\widehat{H}_{i+1} - 2\widehat{H}_i + \widehat{H}_{i-1}\right) - \frac{\Delta t}{2\Delta y\xi(t^n)}\left(\widehat{Q}_{i+1} - \widehat{Q}_{i-1}\right), \\
Q_i^{n+1} - \widehat{Q}_i &= \frac{1}{2}\left(\widehat{Q}_{i+1} - 2\widehat{Q}_i + \widehat{Q}_{i-1}\right) - \frac{\Delta t}{2\Delta y\xi(t^n)}\left(\widehat{M}_{i+1} - \widehat{M}_{i-1}\right) + \\
&\qquad \frac{1}{\Delta y}\int_{t^n}^{t^{n+1}}\int_{y_i-\frac{1}{2}}^{y_i+\frac{1}{2}} -gH(s,\eta)\frac{\partial}{\partial x} z\big(\eta\xi(s)\big)\, d\eta ds.
\end{aligned}$$

Using the conditions of a lake at rest in time t^n *i.e.*, $H_i^n + Z_i^n = C$ and $Q_i^n = 0$, one obtains

$$\left(\frac{\partial H}{\partial y}\right)_i^n + \xi(t^n)\frac{\partial}{\partial x} z(y_i\xi(t_n)) = 0, \quad \left(\frac{\partial^2 H}{\partial y^2}\right)_i^n + \xi(t^n)^2\left(\frac{\partial^2 z}{\partial x^2}\right)_i^n = 0, \quad \left(\frac{\partial Q}{\partial y}\right)_i^n = \left(\frac{\partial^2 Q}{\partial y^2}\right)_i^n = 0.$$

Consider now the equation for H_i^{n+1} and adding and subtracting z_i^{n+1}, $\widehat{Q}_i = 0$ yields

$$\begin{aligned}
H_i^{n+1} + Z_i^{n+1} - Z_i^n + \Delta t (H_y)_i^n \frac{y_i\xi'(t^n)}{\xi(t^n)} &+ \frac{\Delta t^2}{2}\left(\left(\frac{\partial^2 H}{\partial y^2}\right)_i^n \left(\frac{y_i\xi'(t^n)}{\xi(t^n)}\right)^2 + \left(\frac{\partial H}{\partial y}\right)_i^n y_i\xi''(t^n)\right) \\
-\widehat{H}_i + \mathcal{O}(\Delta t^3) &= \frac{1}{2}\left(\widehat{H}_{i+1} - 2\widehat{H}_i + \widehat{H}_{i-1}\right) + \mathcal{O}(\Delta y^3), \\
H_i^{n+1} + Z_i^{n+1} - (H_i^n + Z_i^n) &= -\frac{1}{2}\xi(t^n)^2\left(\frac{\partial^2 z}{\partial x^2}\right)_i^n \Delta y^2 + \mathcal{O}(\Delta y^3).
\end{aligned}$$

Hence, as correction to the overall scheme we need to add to the integration of the equation (3.2)

$$\mathcal{S}_i^n = \frac{\Delta y^2}{2}\xi(t^n)^2\frac{\partial^2}{\partial x^2} z(y_i\xi(t^n)).$$

This leads to a well-balanced discretization up to order $\mathcal{O}(\Delta y^3)$. A similar computation leads to

$$Q_i^{n+1} = -\frac{g\Delta t}{4\Delta y\xi(t^n)}\left(2\left(\frac{\partial\widehat{H}}{\partial y}\right)_i^n \Delta y\right)\left(2\widehat{H}_i + \Delta y^2\left(\frac{\partial^2\widehat{H}}{\partial y^2}\right)_i^n\right) + G_i^n + \mathcal{O}(\Delta y^3),$$

where

$$G_i^n = -\frac{1}{\Delta y}\int_{t^n}^{t^{n+1}}\int_{y_{i-\frac{1}{2}}}^{y_{i+\frac{1}{2}}} gh(s,\eta)\frac{\partial}{\partial x}z(\eta\xi(s))dsd\eta.$$

This leads to

$$Q_i^{n+1} = \frac{g\Delta t}{\Delta y\xi(t^n)}\Delta y\widehat{H}_i^n\frac{\partial}{\partial x}z\left(y_i\xi(t^n)\right)\xi(t^{n+1}) + G_i^n + \mathcal{O}(\Delta y^3),$$

and after further Taylor expansion $\Delta y\frac{\partial}{\partial x}z\left(y_i\xi(t^n)\right)\left(\xi(t^n)+\Delta t\xi'(t^n)\right)\widehat{H}_i^n + \mathcal{O}(\Delta t^2\Delta y)$ and midpoint integration

$$G_i^n = -\frac{g}{\Delta y}\int_{t^n}^{t^{n+1}}\int_{y_{i-\frac{1}{2}}}^{y_{i+\frac{1}{2}}} H(s,\eta)\xi(s)\frac{\partial}{\partial x}z(\eta\xi(s))dsd\eta = -\Delta tg\widehat{H}_i\frac{\partial}{\partial x}z(y_i\xi(t^n), \tag{4.2}$$

one obtains

$$Q_i^{n+1} = \frac{g\Delta t^2\xi'(t^n)}{\xi(t^n)}\frac{\partial}{\partial x}z(y_i\xi(t^n))\widehat{H}_i^n + \mathcal{O}(\Delta y^3).$$

Finally, this leads to the second-order correction term to the momentum equation as

$$\mathcal{Q}_i^n = -\frac{g\Delta t^2\xi'(t^n)}{\xi(t^n)}\frac{\partial}{\partial x}z(y_i\xi(t^n))\widehat{H}_i^n.$$

In summary, at each time step t^n the equation (3.1) is solved using a third-order interpolation on $\mathbf{W}_i^n$ as well as formula (3.6) to obtain the intermediate values $\widehat{\mathbf{W}}_i^n$. Equation (3.2) is discretized as

$$\mathbf{W}_i^{n+1} = \widehat{\mathbf{W}}_i^n - \left(\widehat{\mathbf{F}}_{i+\frac{1}{2}}^n - \widehat{\mathbf{F}}_{i-\frac{1}{2}}^n\right) + \mathbf{G}_i^n + \mathbf{S}_i^n, \tag{4.3}$$

where $\widehat{\mathbf{F}}_{i+\frac{1}{2}}^n$ are the numerical fluxes defined in (3.8), $\mathbf{S}_i^n$ and $\mathbf{G}_i^n$ are source terms defined as

$$\mathbf{G}_i^n = \begin{pmatrix} 0 \\ \\ -\Delta tg\widehat{H}_i\dfrac{\partial}{\partial x}z(y_i\xi(t^n) \end{pmatrix}, \qquad \mathbf{S}_i^n = \begin{pmatrix} \dfrac{\Delta y^2}{2}\xi(t^n)^2\ z_{xx}(y_i\xi(t^n)) \\ \\ -\dfrac{g\Delta t^2\xi'(t^n)}{\xi(t^n)}\dfrac{\partial}{\partial x}z(y_i\xi(t^n))\widehat{H}_i^n \end{pmatrix}.$$

Note that the methods presented are only first-order accurate in space and time. However, higher order schemes can be reconstructed following similar techniques.

5 Numerical results

We present numerical results for several test problems of shallow water flows over dry areas. The main goals of this section are to illustrate the numerical performance of the techniques described above and to verify numerically their capability to solve moving wet/dry fronts in shallow water flows. In all the computations reported herein, the Courant number Cr is set to Cr = 1 and the time stepsize Δt is adjusted at each time step according to the Courant-Friedrichs-Lewy (CFL) stability condition

$$\Delta t^n = \mathrm{Cr}\frac{\Delta y}{\max\left(|\lambda_1^n|, |\lambda_2^n|\right)},$$

where λ_1 and λ_2 are the two eigenvalues of the parametrized shallow water system given by (2.9). We present numerical results obtained using the Lax-Friedrichs, Rusanov, Roe and FVC methods

Table 5.1: Errors in the water height H and the water discharge Q obtained for the accuracy test problem using the parametrized model for the considered finite volume methods at time $t = 1$ using different gridpoints.

	Lax-Friedrich		Rusanov		Roe		FVC	
N	Error in H	Error in Q	Error in H	Error in Q	Error in H	Error in Q	Error in H	Error in Q
100	2.174E-01	8.936E-01	1.791E-01	7.752E-01	1.283E-01	5.108E-01	1.023E-01	3.961E-01
200	1.385E-01	6.318E-01	1.102E-01	4.906E-01	7.628E-02	3.300E-01	5.295E-02	2.274E-01
400	7.683E-02	3.889E-01	5.905E-02	2.740E-01	4.173E-02	2.031E-01	2.470E-02	1.160E-01
800	3.976E-02	2.157E-01	2.952E-02	1.448E-01	1.946E-02	1.058E-01	1.003E-02	5.411E-02

Table 5.2: Errors in the water free-surface $H + Z$ and the water velocity U obtained for the verification of well-balanced property at time $t = 10$ using different gridpoints.

	Standard treatment		Well-balanced treatment	
N	Error in $H + Z$	Error in U	Error in $H + Z$	Error in U
100	3.836E-02	5.924E-02	7.655E-14	8.716E-14
200	2.764E-03	3.783E-03	9.301E-15	1.136E-14

and we also compare the obtained results for the parametrized model (2.5) to those obtained for the original model (2.1) using the same methods. Here, to overcome the zero speeds in the original system, we perturb the associated characteristic speeds by 10^{-9} far from zero. In our simulations presented in this section the gravitational force is set to $g = 9.81\ m/s^2$ and comparisons between different methods are presented. The following test examples are selected:

5.1 Accuracy test example

In this example we investigate the accuracy of the proposed method for the shallow water equations over dry areas. We examine the performance of the considered finite volume methods for the parametrized model (2.5) using different numbers of gridpoints. To this end we consider the problem studied in [28] for the shallow water equations (2.1) in the spatial domain $[0, 1]$ with a non-flat bottom given by

$$z(x) = \sin^2(\pi x), \tag{5.1}$$

and subject to the following initial conditions

$$h(0, x) = 5 + e^{\cos(2\pi x)}, \qquad u(0, x) = 0.$$

Periodic boundary conditions are used for this test example. In order to quantify the errors in this problem a reference solution computed using a fine mesh of 6400 gridpoints is used as an exact solution. We compute the solutions at time $t = 1$ using different mesh densities. We consider the L^1-error norm defined as

$$\sum_{i=1}^{N} |H_i^n - \mathcal{H}_i^n| \, \Delta x, \tag{5.2}$$

where H^n and $\mathcal{H}_i^n$ are respectively, the computed and reference solutions at gridpoint x_i and time t, whereas N stands for the number of gridpoints used in the spatial discretization. The obtained

results for the water height H and the water discharge Q are listed in Table 5.1 using different values of N. By increasing the number of gridpoints in the computational domain, the errors decrease in all considered finite volume methods. A faster decay in the errors is also observed for the errors in the water height compared to the errors in the water discharge for the methods in Table 5.1. The Lax-Friedrichs and Rusanov schemes exhibits errors of the same order whereas an improvement is detected in the errors computed using the Roe scheme. We also remark that for these schemes, nearly optimal convergence rates of first-order are observed in the L^1-error norm for both H and Q. These results also confirm that a finite volume scheme designed for solving the original shallow water equations (2.1) will retain the same order of convergence when it is applied to the parametrized shallow water system (2.5). For this test example, the FVC method is the most accurate and based on the results presented in Table 5.1 the FVC methods is more accurate than the Lax-Friedrichs, Rusanov and Roe schemes. We clearly see that the convergence rates for the FVC method for both H and Q are superior than those obtained using the other methods. Needless to mention that increasing the number of gridpoints N results in an increase of the computational cost in all considered methods. For the considered mesh densities, the required CPU time in the FVC method is more than 5 times lower than the other methods.

Next we check the well-balanced property proposed in the current study. To this end we consider the example of a lake at rest flow using the bed given by (5.1) and a free-surface initially set to 2. It is expected that the water free-surface remains constant and the water velocity should be zero at all simulation times. Here, we run the standard method without accounting for the terms $\mathbf{S}_i^n$ in (4.3) and the well-balanced method including the terms $\mathbf{S}_i^n$ in (4.3). In Table 5.2 we summarize the errors in the water free-surface and the water velocity obtained at time $t = 10$ for both treatments using two different meshes. It is clear that the standard approach fails to exactly conserve a constant free-surface and it introduces large errors in both water free-surface and water velocity for the considered meshes. As can be seen, the water free-surface for the well-balanced approach remains constant during the simulation times and the proposed well-balanced treatment preserves the C-property to the machine precision.

5.2 Dam-break flow over flat dry bed

We consider the dam-break problem in a rectangular channel with flat bottom, $z(x) = 0$. The channel is of length 30 m and the initial conditions are given by (2.1b) with $h_0 = 1$ m and $u_0 = 0$ m/s. At $t = 0$ the dam collapses and the flow problem consists of a shock wave traveling downstream and a rarefaction wave traveling upstream. The analytical solution of this problem is given by [12]

$$h(t,x) = \begin{cases} h_0, & \text{if} \quad x \leq -t\sqrt{gh_0}, \\ \dfrac{1}{9g}\left(2\sqrt{gh_0} - \dfrac{x}{t}\right)^2, & \text{if} \quad -t\sqrt{gh_0} < x \leq 2t\sqrt{gh_0}, \\ 0, & \text{if} \quad x > 2t\sqrt{gh_0}, \end{cases}$$

$$u(t,x) = \begin{cases} 0, & \text{if} \quad x \leq -t\sqrt{gh_0}, \\ \dfrac{2}{3}\left(\sqrt{gh_0} + \dfrac{x}{t}\right)^2, & \text{if} \quad -t\sqrt{gh_0} < x \leq 2t\sqrt{gh_0}, \\ 0, & \text{if} \quad x > 2t\sqrt{gh_0}. \end{cases}$$

In Figure 5.1 we present the evolution in time-space phase domain of the water height obtained for the considered finite volume methods using a mesh with 100 gridpoints. In this figure we

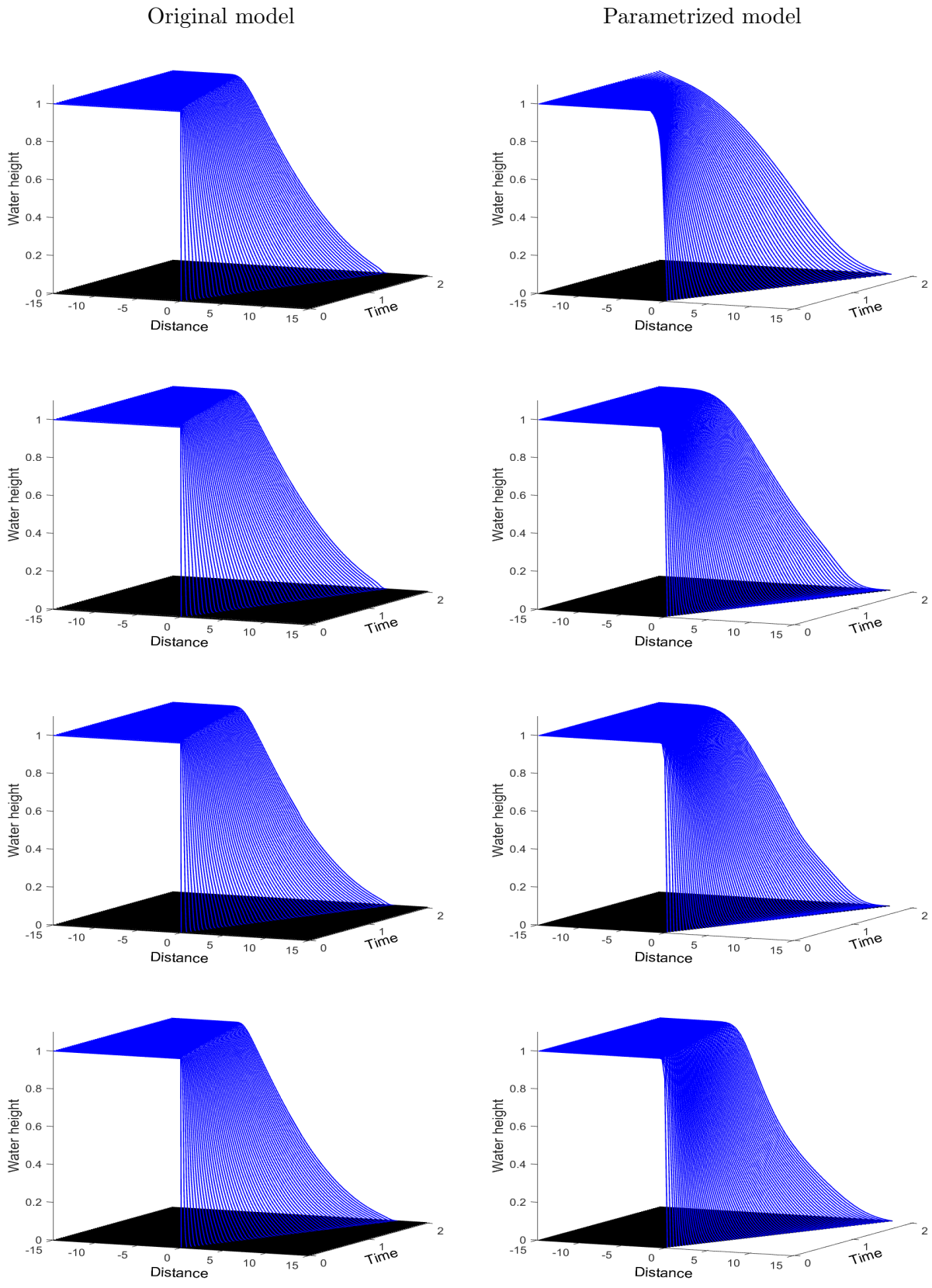

Figure 5.1: Evolution in the time-space domain of the water height for the dam-break over flat bed using the original model (left column) and the parametrized model (right column) for the Lax-Friedrichs method (first row), the Rusanov method (second row), the Roe method (third row) and the FVC method (fourth row) on a mesh with 100 gridpoints.

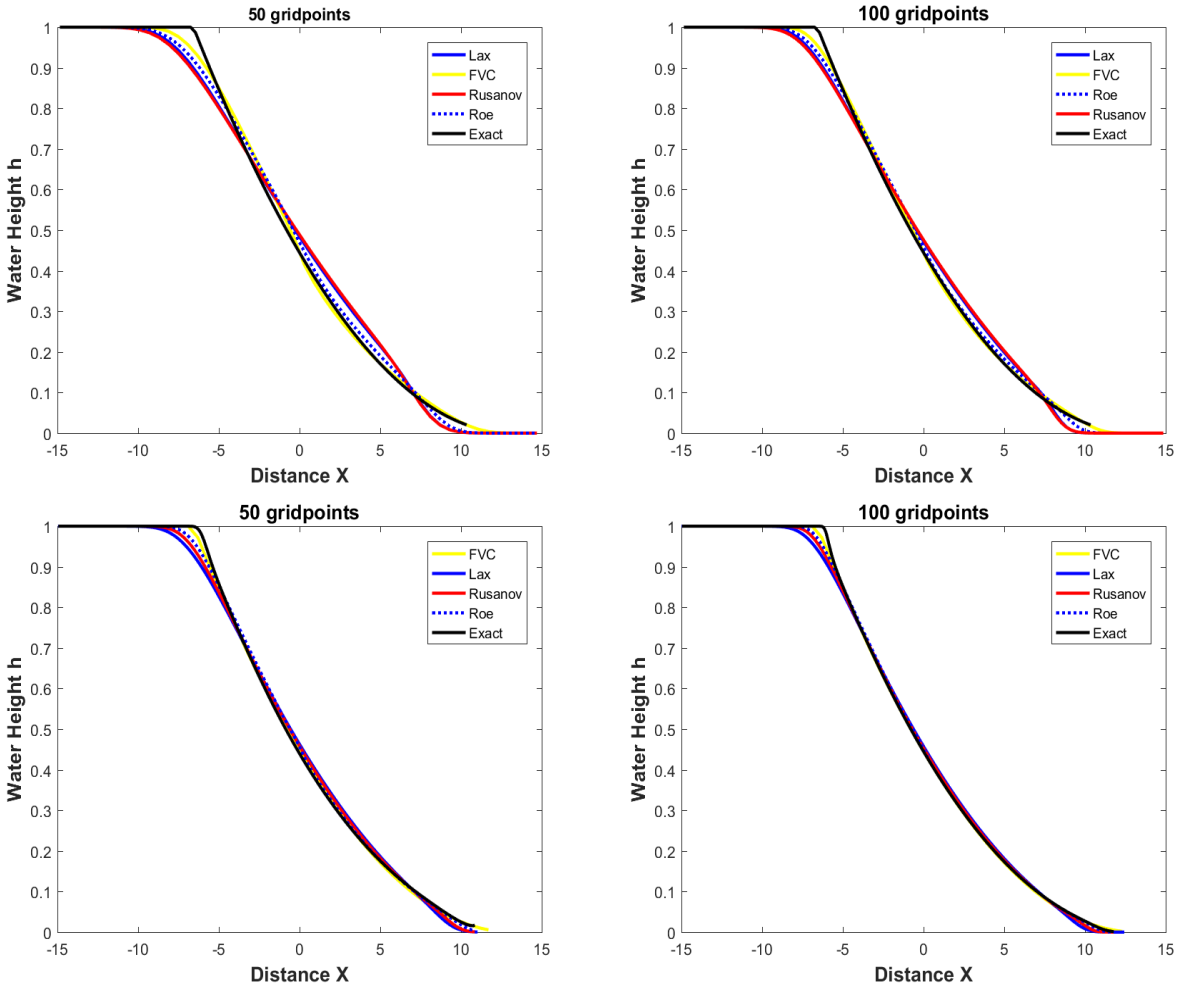

Figure 5.2: Comparison of results obtained for the dam-break over flat bed using the considered finite volume methods for the original model (first row) and the parametrized model (second row) at time $t = 2.1$ using 50 gridpoints (left column) and 100 gridpoints (right column).

include both results obtained for the original model (2.1) and the parametrized model (2.5) using the same number on gridpoints. It is clear that for this dam-break problem, the results obtained using the classical Lax-Friedrichs and Rusanov methods are roughly the same in both original and parametrized models. For both models, the FVC method is more accurate as it is clearly seen in the vicinity of the shock and the contact waves. To further emphasis these features, we display in Figure 5.2 a comparison between the results from Figure 5.1 at time $t = 2.1$ using two meshes with 50 and 100 gridpoints, respectively. It is also clear that for both models, the numerical diffusion is very pronounced in the numerical solutions computed using Lax-Friedrichs and Rusanov methods. This excessive numerical dissipation has been successfully removed in the water heights using the Roe method but the results obtained using the FVC method remain the best. On the other hand, the proposed parametrized model captures the wet/dry fronts more accurately compared to the original approach. For this test example, the combined parametrized model and the FVC method accurately solve the front propagation without generating nonphysical oscillations or excessive numerical dissipation in the computed results.

Next we examine the performance of the original and parametrized models for capturing the moving wet/dry interface in this dam-break flow problem. Note that the wet/dry interface $\zeta(t)$ for

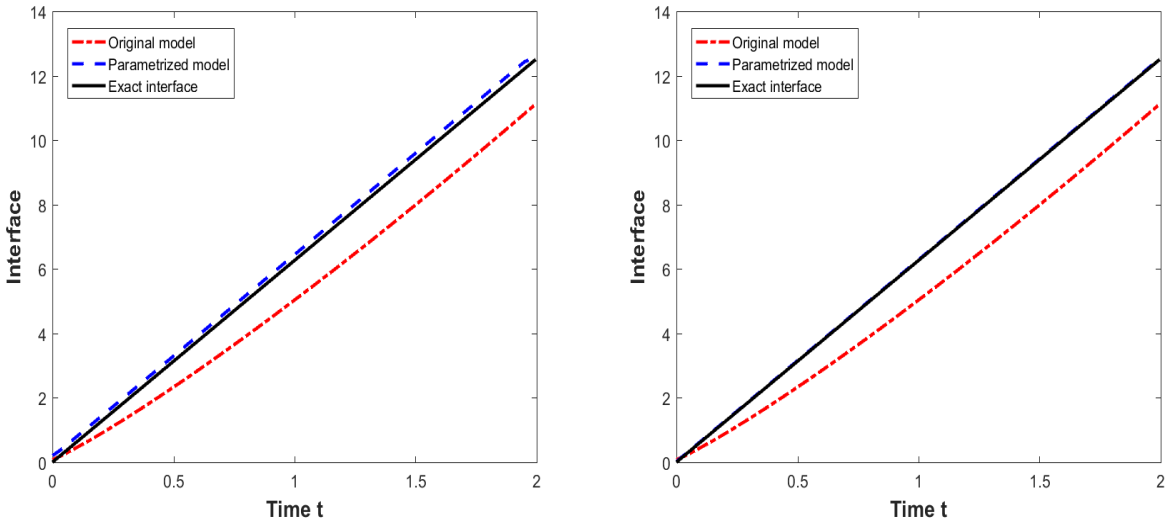

Figure 5.3: Time evolution for the wet/dry front obtained for the dam-break over flat bed using the FVC method for the original and parametrized models using 50 gridpoints (left column) and 100 gridpoints (right column).

Table 5.3: Errors in the wet/dry interface ζ obtained for the dam-break over flat bed using the original and parametrized models for the considered finite volume methods at time $t = 2.1$ using different gridpoints.

	Original model				Parametrized model			
N	Lax-Friedrichs	Rusanov	Roe	FVC	Lax-Friedrichs	Rusanov	Roe	FVC
100	9.550E-01	7.895E-01	5.417E-01	1.351E-01	3.142E-03	2.469E-03	1.406E-03	7.304E-04
200	5.298E-01	4.319E-01	2.902E-01	6.754E-02	1.570E-03	1.151E-03	5.710E-04	2.582E-04
400	2.742E-01	2.204E-01	1.401E-01	2.939E-02	7.324E-04	5.010E-04	2.163E-04	8.517E-05
800	1.324E-01	1.049E-01	6.535E-02	1.113E-02	3.187E-04	2.034E-04	7.647E-05	2.621E-05

this test example can be analytically computed using

$$\zeta\left(t\right) = 2t\sqrt{gh_0}.$$

Figure 5.3 depicts the time evolution of the moving wet/dry interface obtained for the original and parametrized models using the FVC method only. For comparison reasons, we present results obtained on two meshes with 50 and 100 gridpoints. As it can be seen from these results, the wet/dry interfaces obtained by the parametrized model are more accurate than those obtained by the original model. Refining the mesh from 50 gridpoints to 100 gridpoints results in a consistent improvement in the computed results for the parametrized model but not for the original model. Obviously, the computed results verify the stability and the shock capturing properties of the proposed parametrized model. The obtained results using the FVC scheme are also in good agreement with the exact solution for this dam-break problem over dry bed. To quantify the errors in the wet/dry interface for this dam-break problem, we summarize in Table 5.3 the L^2-errors for the considered finite volume methods for both the original and parametrized models. Here we present

Table 5.4: Errors in the wet/dry interface ζ obtained for the dam-break over non-flat bed using the original and parametrized models for the considered finite volume methods at time $t = 2.1$ using different gridpoints.

	Original model				Parametrized model			
N	Lax-Friedrichs	Rusanov	Roe	FVC	Lax-Friedrichs	Rusanov	Roe	FVC
100	9.785E-01	8.936E-01	6.750E-01	2.715E-01	4.692E-03	3.573E-03	2.358E-03	8.903E-04
200	5.620E-01	4.957E-01	3.876E-01	1.454E-01	2.346E-03	1.786E-03	1.026E-03	3.373E-04
400	3.011E-01	2.565E-01	1.938E-01	7.270E-02	1.173E-03	8.331E-04	4.166E-04	1.192E-04
800	1.505E-01	1.238E-01	9.359E-02	3.391E-02	5.472E-04	3.626E-04	1.578E-04	3.932E-05

the errors at time $t = 2.1$ using different numbers of gridpoints. Again, the combined parametrized model with FVC method produced the most accurate results for this example. The performance of the parametrized model and the FVC method is very attractive since the computed solutions remain stable and accurate even for relatively coarse meshes without solving Riemann problems or requiring complicated treatment of wet/dry fronts in the flow problem.

5.3 Dam-break flow over non-flat dry bed

Our next flow problem consists of introducing a non-flat bed in the previous example of dam-break problems over dry beds. We consider an inclined bed with a slope of $\alpha = \frac{\pi}{60}$ defined as

$$z(x) = (15 - x)\tan(\alpha).$$

As in the previous test example, Figure 5.4 illustrates the evolution of the water free-surface in time-space phase domain for the considered finite volume schemes using a mesh with 100 gridpoints. We present numerical results obtained for the original model (2.1) and the parametrized model (2.5) using the same number on gridpoints. As can be seen from these figures, the numerical diffusion is more pronounced in the results obtained using the Lax-Friedrichs and Rusanov methods, compare the plots of the water free-surface for the mesh of 50 gridpoints. As expected, the Roe method has been successful in eliminating the numerical diffusion, but the FVC method is most accurate near regions of large gradients. On the other hand, comparing the performance of the parametrized model and the original method in Figure 5.5, results for the parametrized model are more accurate than those obtained using the original model with a negligible numerical diffusion is introduced compared to the one introduced by the original model. For this test example, no significant differences have been observed between the numerical results obtained using the parametrized model and the analytical solutions. It is also seen that for the considered dam-break conditions, the FVC method gives better results, followed by the Roe scheme.

For the sake of comparison, we illustrate in Figure 5.6 the time evolution of the moving wet/dry interface obtained for the original and parametrized models. For this test example, the exact equation of the interface is defined by

$$\zeta(t) = 2t\sqrt{gh_0\cos(\alpha)} - \frac{gt^2}{2}\tan(\alpha).$$

Only results obtained using the FVC scheme are presented in Figure 5.6. The computed and analytical wet/dry interfaces are virtually indistinguishable for the simulations using the parametrized

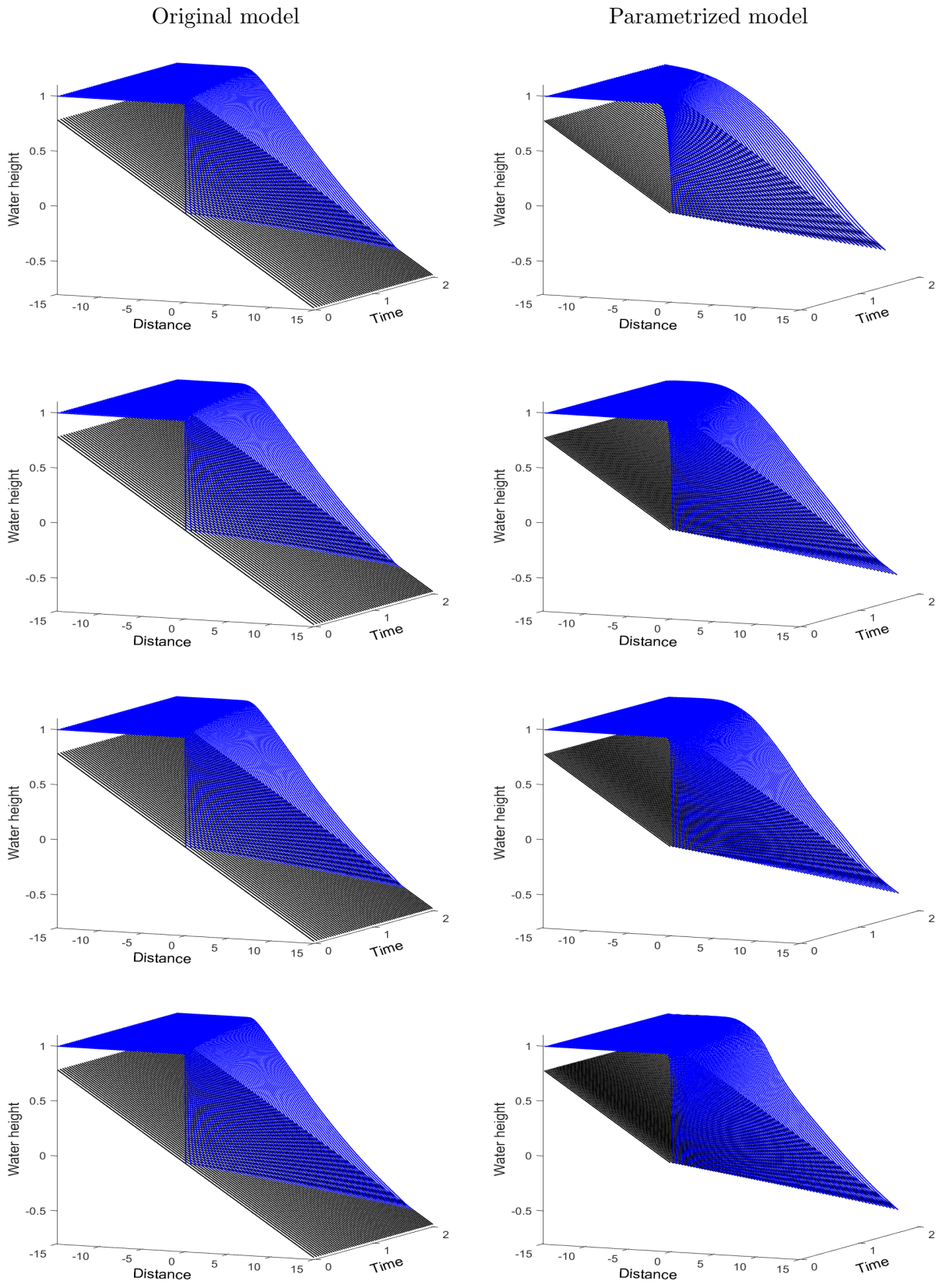

Figure 5.4: Evolution in the time-space domain of the water height for the dam-break over non-flat bed using the original model (left column) and the parametrized model (right column) for the Lax-Friedrichs method (first row), the Rusanov method (second row), the Roe method (third row) and the FVC method (fourth row) on a mesh with 100 gridpoints.

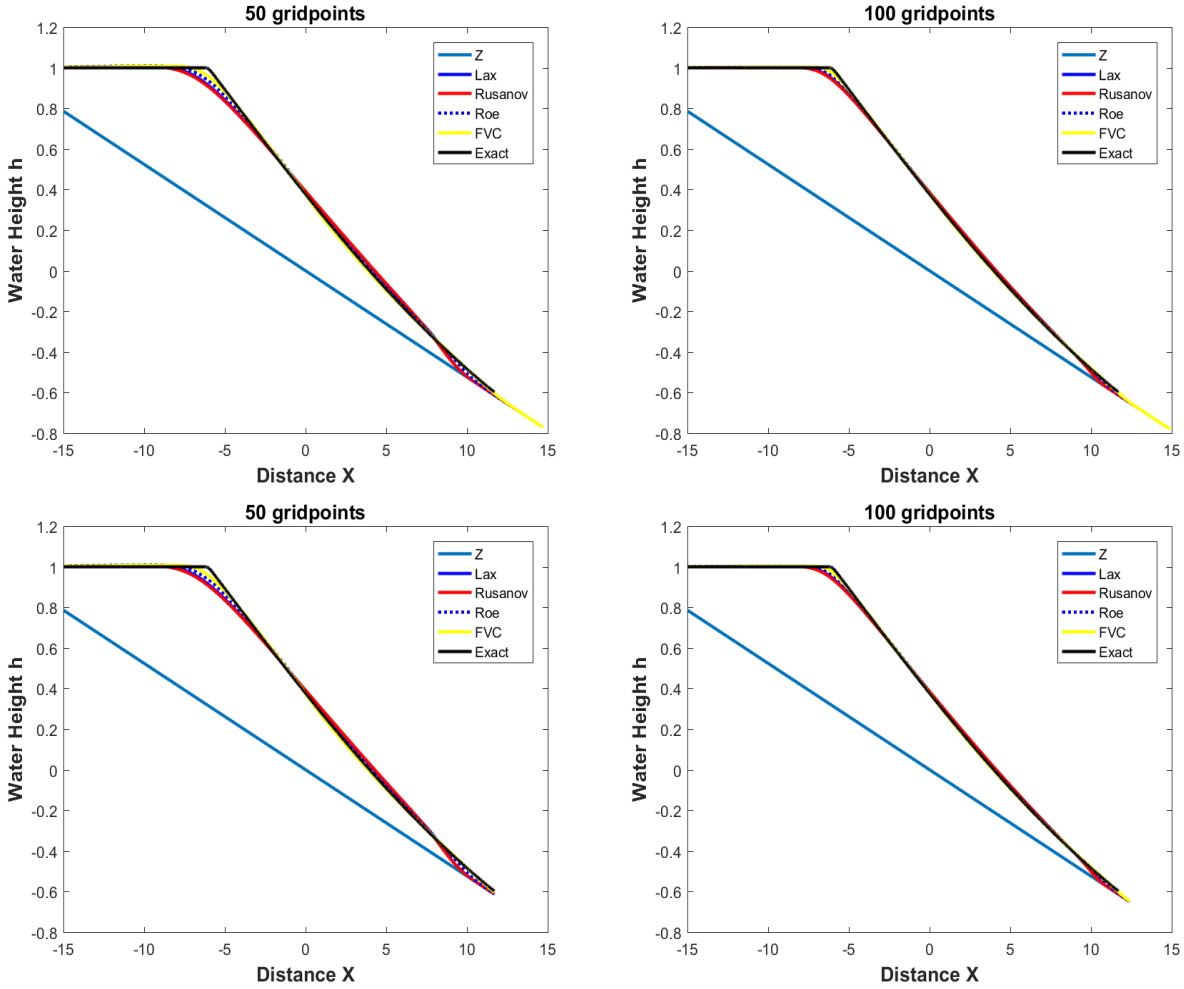

Figure 5.5: Comparison of results obtained for the dam-break over non-flat bed using the considered finite volume methods for the original model (first row) and the parametrized model (second row) at time $t = 2.1$ using 50 gridpoints (left column) and 100 gridpoints (right column).

model on a mesh with 100 gridpoint. A slightly larger errors have been detected in the results obtained for the original model on the same mesh. The FVC method for the parametrized model performs very well for this test problem since it does not diffuse the moving wet/dry fronts and no spurious oscillations have been observed when the water flows over the non-flat bed. The associated L^2-errors in the wet/dry interface are given in Table 5.4 for all considered finite volume schemes at time $t = 2.1$ using different number of gridpoints. It reveals that increasing the number of gridpoints in the computational domain results in a decay of the errors for all methods. Our parametrized model method exhibits good convergence behavior for this dam-break problem over dry bed. As can be seen from the errors presented in Table 5.4, the original model is less accurate in capturing the wet/dry interface than the its parametrized counterpart.

6 Conclusions

In this paper, we have presented a class of accurate well-balanced finite volume methods to solve moving wet/dry fronts in shallow water flows. The method combines the attractive attributes of parameterization techniques and the finite volume discretization to yield a procedure for either

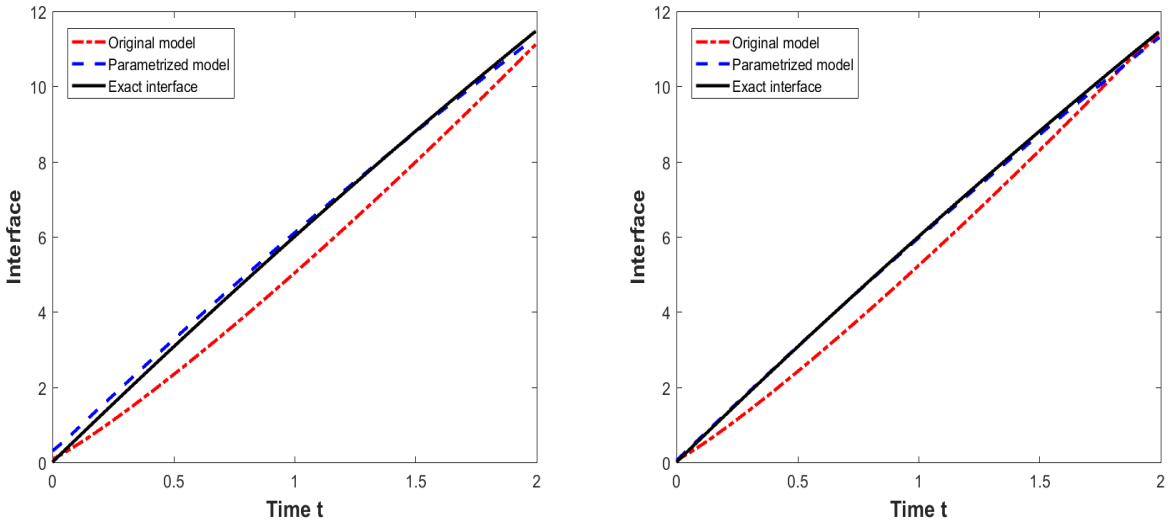

Figure 5.6: Time evolution for the wet/dry front obtained for the dam-break over non-flat bed using the FVC method for the original and parametrized models using 50 gridpoints (left column) and 100 gridpoints (right column).

flat or non-flat topography. We have implemented well-established finite volume methods such as the Lax-Friedrichs and Roe solvers and we have also considered the finite volume characteristics scheme. Combining the new parametrized model with the finite volume characteristics method has several advantages. First, it can solve steady flows over irregular beds without large numerical errors, thus demonstrating that the proposed methods achieve perfect numerical balance of the gradient fluxes and the source terms. Second, it can compute the numerical flux corresponding to the real state of water flow without relying on Riemann problem solvers. Third, reasonable accuracy can be obtained easily and no special treatment is needed to treat moving wet/dry fronts. Finally, the proposed approach does not require either nonlinear solution or special front tracking techniques. Furthermore, it has strong applicability to various shallow water systems as shown in the numerical results. The proposed parametrized finite volume model has been tested on systems of shallow water equations subject to moving wet/dry fronts. The obtained results indicate good shock resolution with high accuracy in smooth regions and without any nonphysical oscillations near the shock areas. Comparisons between the proposed parametrized approach and the conventional shallow water system have also been carried out in this study. For all considered test examples the accuracy of the proposed approach is superior than the original model. Although we have restricted our numerical computations to the low-order methods, the current finite volume scheme can be straightforwardly extended to high-order discretizations. This and further issues are subject of future investigations.

Acknowledgments. This work has been supported by BMBF KinOpt 05M2013 and DFG Cluster of Excellence EXC128. The work of M. Seaid was supported in part by Deutscher Akademischer Austauschdienst (DAAD).

References

[1] E. Audusse, F. Bouchut, M.O. Bristeau, R. Klein, and B. Perthame. A fast and stable well-balanced scheme with hydrostatic reconstruction for shallow water flows. *SIAM Journal on Scientific Computing*, 25:2050–2065, 2004.

[2] F. Benkhaldoun, S. Sari, and Seaid M. A family of finite volume Eulerian-Lagrangian methods for two-dimensional conservation laws. *Journal of Computational and Applied Mathematics*, 285:181–202, 2015.

[3] F. Benkhaldoun and M. Seaid. A simple finite volume method for the shallow water equations. *J. Comp. Applied Math.*, 234:58–72, 2010.

[4] A. Bermudez and M.E. Vázquez-Cendón. Upwind methods for hyperbolic conservation laws with source terms. *Computers & Fluids.*, 23:1049–1071, 1994.

[5] J. Birman, A. Falcovitz. Application of the grp scheme to open channel flow equations. *J. Comput. Phys.*, 222:131–154, 2007.

[6] A. Bollermann, G. Chen, A. Kurganov, and S. Noelle. A well-balanced reconstruction of wet/dry fronts for the shallow water equations. *Journal of Scientific Computing*, 56:267–290, 2013.

[7] A. Bollermann, S. Noelle, and M. Lukácová-Medvidová. Finite volume evolution Galerkin methods for the shallow water equations with dry beds. *Communications in Computa1tional Physics*, 10:371–404, 2001.

[8] F. Bouchut. *Nonlinear Stability of Finite Volume Methods for Hyperbolic Conservation Laws and Well-Balanced Schemes for Sources.* Birkhäuser, Basel, 2004.

[9] M. Brocchini and N. Dodd. Nonlinear shallow water equations modeling for coastal engineering. *J. Waterw. Port, Coastal, Ocean Eng.*, 134:104–120, 2008.

[10] S. Chen, G. Noelle. A new hydrostatic reconstruction scheme based on subcell reconstructions. *SIAM J. Numer. Anal.*, 55:758–784, 2017.

[11] A.J.C. de Saint-Venant. Théorie du mouvement non permanent des eaux, avec application aux crues des riviére at á l'introduction des warées dans leurs lits. *Comptes Rendus des séances de l'Académie des Sciences*, 73:237–240, 1871.

[12] A. Ern, S. Piperno, and K. Djade. A well-balanced Runge-Kutta discontinuous Galerkin method for the shallow water equations with flooding and drying. *Int. J. Numer. Meth. Fluids*, 58:125, 2008.

[13] J.M. Gallardo, C. Parés, and M. Castro. On a well-balanced high-order finite volume scheme for shallow water equations with topography and dry areas. *Journal of Computational Physics*, 227:574–601, 2007.

[14] J. Glimm, G. Marshall, and B. Plohr. A generalized riemann problem for quasi-one-dimensional gas flows. *Adv. in Appl. Math.*, 5:1–30, 1984.

[15] R. J. LeVeque. *Finite volume methods for hyperbolic problems.* Cambridge Texts in Applied Mathematics. Cambridge University Press, 2002.

[16] R.J. LeVeque. *Numerical Methods for Conservation Laws.* Lectures in Mathematics, ETH Zürich, 1992.

[17] R.J. LeVeque. Balancing source terms and fux gradients in high-resolution Godunov methods: the quasi-steady wave-propagation algorithm. *Journal of Computational Physics*, 146:346–365, 1998.

[18] G. Li, J. Chen. The generalized riemann problem method for the shallow water equations with bottom topography. *J. Numer. Methods Engrg.*, 65:834–862, 2006.

[19] Y. Li and F. Raichlen. Non-breaking and breaking solitary wave run-up. *J. Fluid Mech.*, 456:295–318, 2002.

[20] S. Noelle, N. Pankratz, G. Puppo, and Natvig. J.R. Well-balanced finite volume schemes of arbitrary order of accuracy for shallow water flows. *Journal of Computational Physics*, 213:474–499, 2006.

[21] P. Roe. Approximate Riemann solvers, parameter vectors, and difference schemes. *Journal of Computational Physics*, 43:357–372, 1981.

[22] J.J. Stoker. *Water Waves.* Interscience Publishers, Inc., New York, 1986.

[23] C. Temperton and A. Staniforth. An efficient two-time-level semi-Lagrangian semi-implicit integration scheme. *Quart. J. Roy. Meteor. Soc.*, 113:1025–1039, 1987.

[24] V.V. Titov and C.E. Synolakis. Numerical modeling of tidal wave run-up. *J. Waterw., Port, Coast., Ocean Engrg.*, 124:157–171, 1998.

[25] E.F. Toro. The dry-bed problem in shallow-water flows. Technical Report No. 9007, College of Aeronautics Reports, 1990.

[26] E.F. Toro. *Shock-capturing methods for free-surface shallow flows.* Wiley, 2002.

[27] C.B. Vreugdenhil. *Numerical Method for Shallow Water Flow.* Kluwer Academic, Dordsecht, 1994.

[28] Y. Xing and C.W. Shu. High order finite difference WENO schemes with the exact conservation property for the shallow water equations. *J. Comp. Physics.*, 208:3206–227, 2005.

[29] F. Zhou, G. Chen, Y. Huang, and H. Feng. An adaptive moving finite volume scheme for modeling flood inundation over dry and complex topography. *Water Resources Research*, 49:1914–1928, 2013.